AD NUMBER

AD232567

NEW LIMITATION CHANGE

TO

Approved for public release, distribution unlimited

FROM

Distribution authorized to U.S. Gov't. agencies and their contractors; Administrative/Operational Use; 14 JAN 1960. Other requests shall be referred to Naval Ordnance Systems Command, Washington, DC 20362.

AUTHORITY

USNOL ltr dtd 29 Aug 1974

UNCLASSIFIED

NAVORD REPORT 6039

10

THE LIFT AND DRAG ON A ROTATING CYLINDER IN SUPERSONIC CROSSFLOW

14 January 1960

U. S. NAVAL ORDNANCE LABORATORY

WHITE OAK, MARYLAND

625200

NAVORD Report 6039

Aerodynamics Research Report 29

THE LIFT AND DRAG ON A ROTATING CYLINDER IN SUPERSONIC CROSSFLOW

Prepared by:

R. T. Hall

ABSTRACT: Experimental results are presented of the lift (Magnus force) and drag on a rotating cylinder in supersonic crossflow. The data were obtained using smooth and roughened, ~~two~~-dimensional 3-inch diameter cylinders. The rotating cylinder was tested at Mach numbers 1.7[illegible] 2.15, 2.48, and 3.24 over a Reynolds number range from 0.55 x 10^6 to 1.06 x 10^6. Rotational speeds of the model were continuously varied from 0 - 400 cps. The Naval Ordnance Laboratory Supersonic Tunnel No. 1 was used for this investigation.

A discussion of the data is presented in which variations within the ~~three~~ parameters (Mach number, rotational speed, and Reynolds number) are shown along with magnitudes of the lift and drag. A further review of the data presents possible correlations with similar subsonic data.

Published February 1960

U. S. NAVAL ORDNANCE LABORATORY
WHITE OAK, MARYLAND

This program was conducted under the sponsorship of the Bureau of Ordnance (ReO) as a part of their basic aerodynamic research program on Magnus effects. The program was completed under task number 803-767/73003/01040.

JOHN A. QUENSE', Acting
Captain, USN
Commander

R. KENNETH LOBB
By direction

CONTENTS

ILLUSTRATIONS

SYMBOLS

a	free-stream speed of sound, ft/sec ($=\sqrt{\gamma RT}$)
a_t	speed of sound at stagnation conditions, ft/sec ($=\sqrt{\gamma RT_t}$)
A_D	drag coefficient reference area, ft^2 (= 3.94)
A_L	lift coefficient reference area, ft^2 (= 3.00)
C_D	drag coefficient ($= F_D/qA_D$)
C_L	lift coefficient ($= F_L/qA_L$)
D	model diameter, ft (= 0.25)
F_D	drag force, lbs
F_L	lift force (Magnus force), lbs
M	free-stream Mach number
n	rotational speed, cps
P_S	free-stream static pressure, lbs/ft^2
P_t	free-stream stagnation pressure, lbs/ft^2
q	free-stream dynamic pressure, lbs/ft^2 ($=\gamma P_S M^2/2$)
R	gas constant (= 1716 $ft^2/sec^2\ {}^oR$)
Re	free-stream Reynolds number, based on model diameter, D
T_S	free-stream static temperature, ^oR
T_t	free-stream stagnation temperature, ^oR
u	tangential velocity of point on surface of the cylinder, ft/sec ($=\pi Dn$)
V	free-stream air velocity, ft/sec
γ	ratio of specific heats (= 1.4 for air)
ρ	free-stream air density, lbs sec^2/ft^4

THE LIFT AND DRAG ON A ROTATING CYLINDER IN SUPERSONIC CROSSFLOW

Introduction

1. The flow about cylinders normal to an airstream has been the subject of considerable analytical and experimental analyses for many years. Many of the concise, mathematical, potential flow analyses have been formulated using a cylinder in a perfect fluid crossflow.

2. From the mathematical concept, when such a cylinder is placed in a two-dimensional, potential crossflow, no net lift force results. This is also true for a viscous, incompressible, homogeneous fluid. Although the boundary layer is considered for this type of fluid, the vortices which are shed (which induce circulation and thus lift) are shed symmetrically and are of opposite sign. Therefore, the net lift is still zero.

3. However, when the cylinder is placed in an airstream and is spun about its axis, a net lift force is produced which is normal to both the airstream and the axis of rotation. This aerodynamic phenomenon is known as the "Magnus effect" after the German scientist who carried out the first experiments which qualitatively proved the existence of such a force.

4. This program was run in order to determine the lift (Magnus force) and drag on a rotating cylinder in supersonic crossflow. The data were obtained at Mach numbers of 1.75, 2.15, 2.48, and 3.24.

Historical Sketch

5. The effect now known as the "Magnus effect" was first observed sometime in the eighteenth century. During that time it was noted that cannon balls exhibited a dispersion which could not be explained (references (1) and (2)). In 1852, Professor Magnus (hence the term Magnus) was assigned the task of finding if a force due to rotation did exist (reference (3)). The proof of such a force was established, but no measurements of magnitude were made. It was not until the 1870's that a plausible theory was advanced. By using the superposition of two different potential flow fields, Lord Rayleigh presented a mathematical picture concerning the irregular flight of a tennis ball (reference (4)). This classic formulation appears in today's theoretical textbooks (references (5-9)). From then until now the "Magnus effect" has received only sporadic attention from both experimental and theoretical fields (references (10-23)).

6. In the 1940's, ballisticians began placing more attention to the aerodynamics involved in the dynamic stability of spinning shells (reference 24). As a result of this, the "Magnus effect" has received much more organized and consistent consideration in the past 15 years (references (25-32)).

7. However, even after many years of work, no fully satisfactory method has been found for predicting Magnus forces.

Objectives of the Test

8. The prime purpose of the program was to extend, experimentally, the two-dimensional subsonic Magnus force on a rotating cylinder in crossflow into the supersonic flow regions.

9. Qualitative and quantitative results were desired for aerodynamic design and to provide experimental data for Magnus force theories which are being developed at the present time.

10. Finally, it was desired to determine if any correllation or parallelism exists between the subsonic and supersonic Magnus force phenomenon.

Some Design Considerations

11. Although, to the author's knowledge, no analytical or experimental data on spinning cylinders in compressible crossflow have been published, previous work from ballistic ranges, wind-tunnels, and theory have dictated two important criteria for any undertaking of experimental Magnus work. These criteria are as follows:

a. A force-sensitive system strong enough to withstand ordinary lift and drag forces, yet sensitive enough to detect accurately the small Magnus forces.

b. A system for spinning the model, small enough to fit inside the model, but powerful enough to rotate the model at very high spin rates.

12. Fortunately, the rapid advances and refinements in Magnus instrumentation at the Naval Ordnance Laboratory (references (33) and (34)) within the past five years have solved the above requirements by the development of:

a. The internally mounted strain-gage balance.

b. Small Air turbines.

13. In connection with this program, a critical problem arose during the early design work for the models. In order to optimize the model system it was necessary to know what loads were to be expected. Due to the lack of experimental data and analytical approaches for predicting the aerodynamic loads, certain assumptions were made:

a. That the lift (Magnus force) would be at least one order of magnitude lower (and very conceivably two orders of magnitude lower) than the drag on the cylinder in crossflow.

b. That the drag would not change appreciably with spin (since, for a blunt body in a supersonic stream the greater portion of its drag is wave drag), and thus the limited drag data available for non-spinning cylinders (reference (35)) in supersonic crossflow could be used in estimating the drag.

14. From the drag estimation, the magnitude of the lift could then be estimated using assumption (a) above.

Model and Balances

15. The model, (Figures 1 and 2) used in this test may be divided into three main sections:

a. The rotating section

b. The stationary section

c. The air-coaster turbine

16. The rotating section is a hollow thin-walled aluminum tube, twelve inches long and three inches in diameter. The model had two interchangeable rotating sections. One rotating section was smooth, (number 32 machine finish) while the other rotating section was roughened by knurling ten inches of the cylinder length. The knurls were approximately 0.007 inches deep. The cylinder was built to a roundness tolerance of 0.001 inch. A steel shaft runs through the center of the cylinder and extends into the stationary sections.

17. The stationary sections, one at each end of the cylinder, are also constructed of aluminum and are three inches in diameter. These sections house the bearings, the air-coaster turbines, and the tachometers.

18. The air-coaster turbine derives its name from the manner in which it is used. The turbine is designed to "power up" the model to some high rotational speed. Then the air to the turbine is shut off, the tunnel started, and the model is allowed to coast to a stop during the blow. Data are taken during the "coasting" period. The turbine has two main parts, the nozzle and the turbine wheel. The high pressure (150 psi) air is piped into the annular ring formed by the bearing support and the nozzle, both of which remain stationary during operation. The air goes through the nozzle and then through the turbine wheel (which is fixed to the shaft and thus the rotating cylinder) and is exhausted through the cylinder to the airstream. Figure 3 shows the model mounted in the wind tunnel.

19. The model, when assembled, spans the wind tunnel in the horizontal plane. Its physical location is approximately the center of the test region formed by the open-jet test section. A model which spans the wind-tunnel nozzle is used in order to approach, as close as possible, two-dimensional flow.

20. The balances are typical strain-gage balances with slight modifications in design. There are two pitch sections four inches apart, which straddle the diameter of the cylinder. Further aft, in a plane normal to the axis of the pitch balances, are the drag sections. The balances were designed using the load estimations previously described. The estimates made, for a Mach number of 2, were F_D = 310 lbs., F_L (Magnus force) = 5 lbs. The drag coefficient is based on frontal area.

Test Instrumentation

21. Two main readout systems are necessary for recording the data. These systems are as follows:

a. Strain-gage readout system.

b. Rotational speed readout system.

22. The strain-gage readout system was composed of dry cell batteries to supply d.c. power to the gages; a nulling unit to balance the bridges and for calibration purposes; a Leeds and Northrup amplifier system for signal amplification and visual observation; an analog computer for automatically computing the desired coefficients; and a Leeds and Northrup X_1, X_2, Y recorder, where the data, in coefficient form were recorded.

23. The rotational speed readout system was composed of a tachometer, mounted inside of the model to detect rotation; an audio oscillator for speed calibration of the recorder chart; an amplifier for signal amplification; and a frequency meter to convert the variable frequency from the tachometer and oscillator to a d.c. voltage which varies proportionally with the frequencies. The output of the frequency meter was used for the input to the Y component of the Leeds and Northrup X_1, X_2, Y recorder. A Berkeley EPUT meter and a three-inch oscilloscope was used for visual monitoring of the rotational speed.

24. The two systems were "brought together" at the Leeds and Northrup X_1, X_2, Y recorder. Here the strain-gage system output was used for X_1 and X_2 inputs, and the speed recording system output was used as the Y input. Thus the final data were displayed as a continuous trace of force (abscissa) versus rotational speed (ordinate).

Test Technique, Data Reduction, and Results

25. A limited wind-tunnel program was planned to investigate the Magnus forces on rotating cylinders at supersonic speeds. The following possible test variables were considered important. Reynolds number, Mach number, rotational speed, and surface roughness. The major parameter was Mach number. The rotational speed was varied from 0 to 400 cps.

26. The data, as presented in this paper, were obtained during several test periods. It was determined that the repeatability of lift forces was within 5 percent.

27. The data obtained were in the form of continuous traces of rotational speed (cps) versus forces (lbs). These traces exhibited some oscillations. Traces having identical variables are grouped together, and data are then averaged for the various runs. The average values are shown plotted as a solid curve through the test points.

28. The Mach numbers and associated Reynolds number are based on free-stream conditions. The Reynolds number is based on the diameter of the cylinder.

29. The lift coefficient is based on the frontal area of the rotating portion of the cylinder since the stationary portion of the cylinder in the airstream does not contribute to the lift.

30. The velocity ratio, u/V, for each Mach number was obtained from the supply temperature, test section calibrations, and the compressible flow tables (reference 36). The tangential velocity, u, of the cylinder was determined by the expression $u = \pi Dn$ for various n's.

31. The drag coefficient is calculated using a frontal area equal to the model diameter times the nozzle width. Corrections for the areas of the model enveloped by the nozzle boundary layer and the free jet mixing layer were not made because the good repeatability and the good agreement with data of reference (35) indicate that the effect is negligible.

32. Several checks were made to determine if the velocity was two-dimensional. These checks were made several ways:

a. A pressure tube was mounted about 3/4-inch behind the model and readings were taken for both the no-spin and spinning conditions.

b. Temporary end plates were mounted on the model and the lift readings were compared with the data for no-end plates present.

c. The drag coefficients obtained during the tests were compared with two-dimensional drag data on cylinders in cross-flow as found in the literature.

33. Figure 4 is a drawing showing the sign convention used throughout the test.

34. Figures 5 through 8 are plots of the rotational speed (cps) vs. the lift coefficient C_L at Mach numbers of 2.15, 2.48, and 3.24 for the smooth cylinder.

35. Figure 9 is a plot of C_L vs. Mach number for the smooth cylinder. In this plot the rotational speed, cps, is used as a parameter.

36. Figure 10 is a plot of the lift coefficient C_L vs. velocity ratio u/V for the smooth cylinder. This figure is a summary plot of the average lift coefficients vs. the velocity ratio with Mach number as a parameter.

37. Figure 11 is a summary of the drag data obtained with the smooth cylinder. This figure is a plot of rotational speed, cps, vs. drag coefficient, C_D. The no-spin drag coefficients are shown as points on the n = 0 line. The curves drawn from these points represent the drag coefficient as a function of spin rate for each of the four Mach numbers tested. Here it may be seen that the earlier assumption that the drag would be insensitive to spin is essentially substantiated.

38. The curve of the drag coefficient C_D (no spin) vs. Mach number is presented in Figure 12. Also shown on this plot, for calibration purposes, are the data from reference (35). Included in this figure are the data obtained with a roughened cylinder. The roughened cylinder was tested at Mach numbers 1.75, 2.15, and 2.48. Only data obtained at Mach number 1.75 were usable due to model and instrumentation difficulties.

39. Figure 13 is a plot of the lift coefficient C_L vs. the velocity ratio, u/V, and Mach number 1.75 for the roughened and the smooth cylinder. The data from the roughened cylinder show an appreciable difference in comparison with data from the smooth cylinder. The roughened cylinder shows an average of 20 percent more lift than does the smooth cylinder.

Conclusions

40. From the preceding discussions the following conclusions may be drawn:

a. The magnitudes of forces and slopes are small when compared to subsonic data. The maximum lift coefficient obtained in the test program was $C_L = 0.009$, which occurred at a Mach number of 2.15. Up to about 200 cps the lift coefficient is linear with increasing rotational speed, and the initial slope values $dC_L/d(u/V)$, were approximately 0.086 with the exception of the data obtained at M = 1.75.

b. All of the curves show (or tend to show) that a maximum lift coefficient is reached at spin ratios of ($1.0 \leq u/V \leq 2.0$). Beyond the point of maximum lift, a loss of lift is experienced for increasing spin up to 400 cps.

c. In spite of smaller magnitudes of lift and slopes, the data show that a qualitative parallelism may exist in a comparison of the Magnus phenomenon in incompressible (reference 31 and 32) and compressible flow.

d. The drag is shown to be very nearly independent of the spin rate; the maximum variation is approximately 3 percent up to 400 cps.

e. Although an appreciable difference in aerodynamic coefficients is shown between the roughened and the smooth cylinder, it is felt that the result at only one Mach number does not justify applying the results over the entire supersonic Mach number range.

REFERENCES

1. Buford, W. D. "Magnus Effect in the Case of Rotating Cylinders and Shells," Memorandum Report No. 821. Ballistics Research Laboratories, July 1954.

2. Robins, B., "New Principles of Gunnery," London: 1842.

3. Magnus, G., "Ueber die Abweichung der Geschosse," Abhandly d. Kig. Akad d. Wiss zu Berlin: 1852.

4. Lord Reyleigh, "On the Irregular Flight of a Tennis Ball," Messenger of Mathematics, VII, 14, 1877.

5. Glauert, H., "Aerofoil and Airscrew Theory," Cambridge: University Press; New York: MacMillan, 1926.

6. Goldstein, Sidney, ed. "Modern Developments in Fluid Dynamics, I, II," Oxford: Claredon Press, 1938.

7. Lamb, H., "Hydrodynamics," New York: Dover Publications.

8. Rauscher, Manfred, "Introduction to Aeronautical Dynamics," New York: John Wiley, 1953.

9. Von Karman, T., "Aerodynamics," New York: Cornell U. Press, 1954.

10. Reid, E. G., "Tests of Rotating Cylinders," NACA Technical Note No. 209, December 1924.

11. Betz, A., "The Magnus Effect,""The Principle of the Flettner Rotor," Translated in NACA Technical Memorandum No. 310.

12. Thom, "Experiments on the Air Forces on Rotating Cylinders," ARC R and M No. 1018, 1925.

13. Thom, "The Pressures Round a Cylinder Rotating in an Air Current," ARC R and M No. 1082, 1926.

14. Thom, "Experiments on the Flow Past a Rotating Cylinder," ARC R and M No. 1410, 1931.

15. Prandtl, L., "Application of the Magnus Effect to the Wind Propulsion of Ships," Translated in NACA Technical Memorandum No. 367, June 1926.

16. Ackeret, J., "Recent Experiments at the Gottingen Aerodynamic Institute," Translated in NACA Technical Memorandum No. 323, July 1925.

17. Bairstow, L. "The Rotorship and Aerodynamics," Nature, CXV, No. 2891, March 28, 1925, pp. 426-464.

18. L. B., Nature, CXIV, No. 2873, November 22, 1924, p. 758.

19. Wolff, E. B., and Koning, C. "Tests for Determining the effect of a Rotating Cylinder Fitted in the Leading Edge of an Airplane Wing," Translated in NACA Technical Memorandum No. 354, March 1926.

20. Wolff, E. B., and Koning, C. " Discussion of the Results of the Boundary-Layer Tests of an Airfoil Fitted with a Rotary Cylinder," Translated in NACA Technical Memorandum No. 424, August 1927.

21. Prandtl, L., and O. Tietjens, "Kinematographic Flow Pictures," Translated in NACA Technical Memorandum No. 364, May 1926.

22. Rizzo, F. "The Flettner Rotor Ship in the Light of the Kutta-Joukowski Theory and of Experimental Results," NACA Technical Notes No. 228, October 1925.

23. Ahlborn, F. "The Magnus Effect in Theory and Reality," Translated in NACA Technical Memorandum No. 567.

24. Kelly, H., and E. McShane, "On the Motion of a Projectile with Small of Slowly Changing Yaw," Ballistic Research Report No. 446, January 1944.

25. Davies, J. "The Aerodynamics of Golf Balls," Journal of Applied Physics, XX, 9, September 1949, pp. 821-828.

26. "Camera and Science Settle the Old Rhubarb about Base-Ball's Curve Ball," Life, XXXV, July 27, 1953, pp. 104-107.

27. Smith, S. "Watch Those Curves," Argosy, CCCXLII, 3, March 1956, p. 41.

28. Martin, J. C. "On Magnus Effects Caused by the Boundary Layer Displacement Thickness on Bodies of Revolution at Small Angles of Attack," Ballistic Research Laboratory Report No. 870, June, 1953.

29. Kelly, Howard R. "An Analytical Method for Predicting the Magnus Forces and Moments on Spinning Projectiles," U. S. Naval Ordnance Test Station Technical Memorandum No. 1634, August 12, 1954.

30. Krahn, E. "Negative Magnus Force," Journal of Aeronautical Sciences, XXIII, 4, April 1956.

31. Van Aken, R., and H. Kelly, "The Magnus Force of Spinning Cylinders," IAS Reprint No. 712, Presented at the 25th Annual Meeting, January 28 - 31, 1957.

32. Swanson, W. M., "An Experimental Investigation of the Two-Dimensional Magnus Effect," Cleveland, Ohio: Case Institute of Technology, December 31, 1956.

33. Shantz, I., Gilbert, B., and White, C., "NOL Wind-Tunnel Internal Strain-Gage Balance Systems," NAVORD Report 2972.

34. Cornett, R., "Design of a Miniature High Speed Air Turbine for Spinning Wind Tunnel Models," Master's Thesis, Department of Mechanical Engineering, University of Maryland, 1955.

35. Hoerner, S. F., "Aerodynamic Drag," The Otterbein Press, 1951, p. 223.

36. Ames Research Staff, "Equations, Tables, and Charts for Compressible Flow," NACA Report 1135, 1953.

PHOTOGRAPH OF "EXPLODED" ROTATING CYLINDER

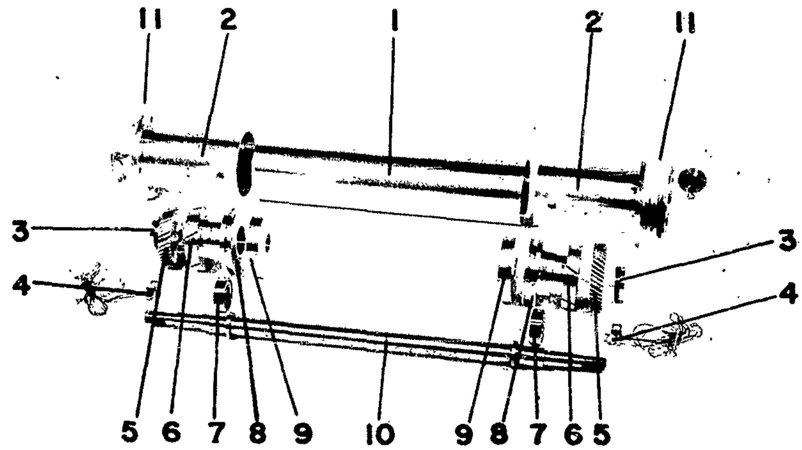

1. CYLINDER (rotating section)
2. CYLINDER (stationary section)
3. TURBINE RETAINING NUT & RING MAGNET
4. TACHOMETER COIL
5. TURBINE WHEEL
6. NOZZLE
7. BEARING
8. END PLATE & BEARING HOLDER
9. END PLATE (rotating section)
10. STEEL SHAFT
11. BALANCE & MODEL HOLDER

FIG. 1

ASSEMBLY DRAWING OF ROTATING CYLINDER

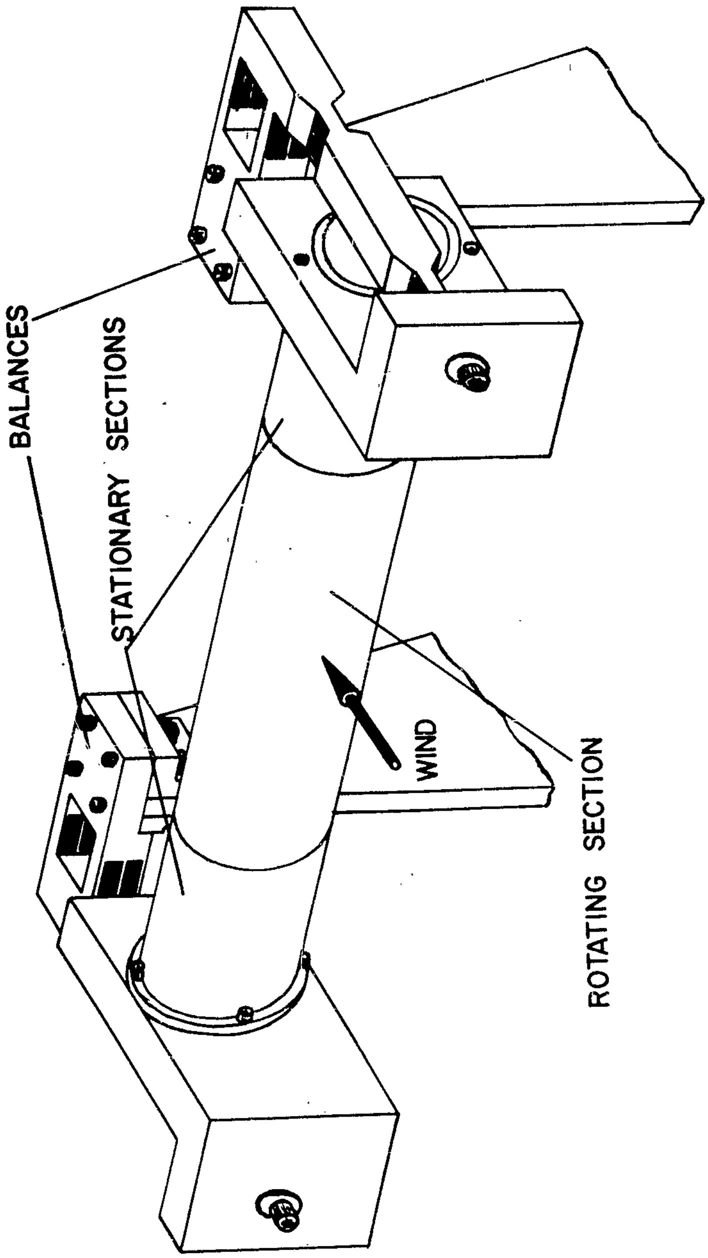

FIG. 2

PHOTOGRAPH OF ROTATING CYLINDER MOUNTED IN WIND TUNNEL

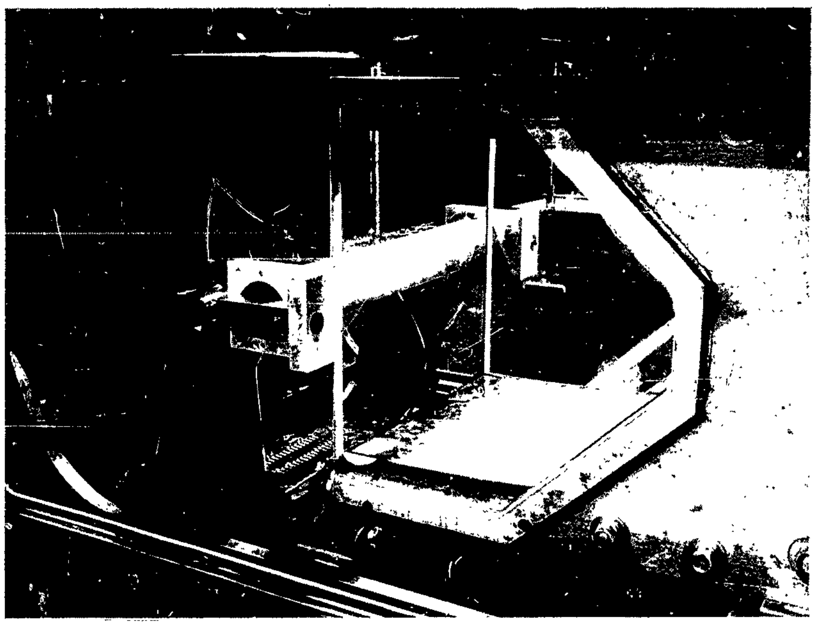

FIG. 3

NAVORD REPORT 6039

SIGN CONVENTION

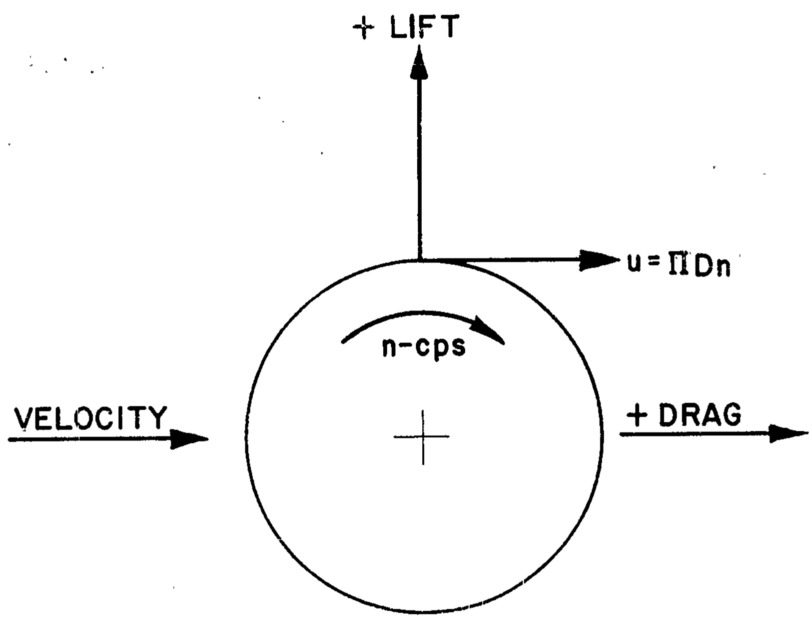

FIG. 4

LIFT COEFFICIENT versus ROTATIONAL SPEED

$Re = 1.06 \times 10^6$

$M = 1.75$

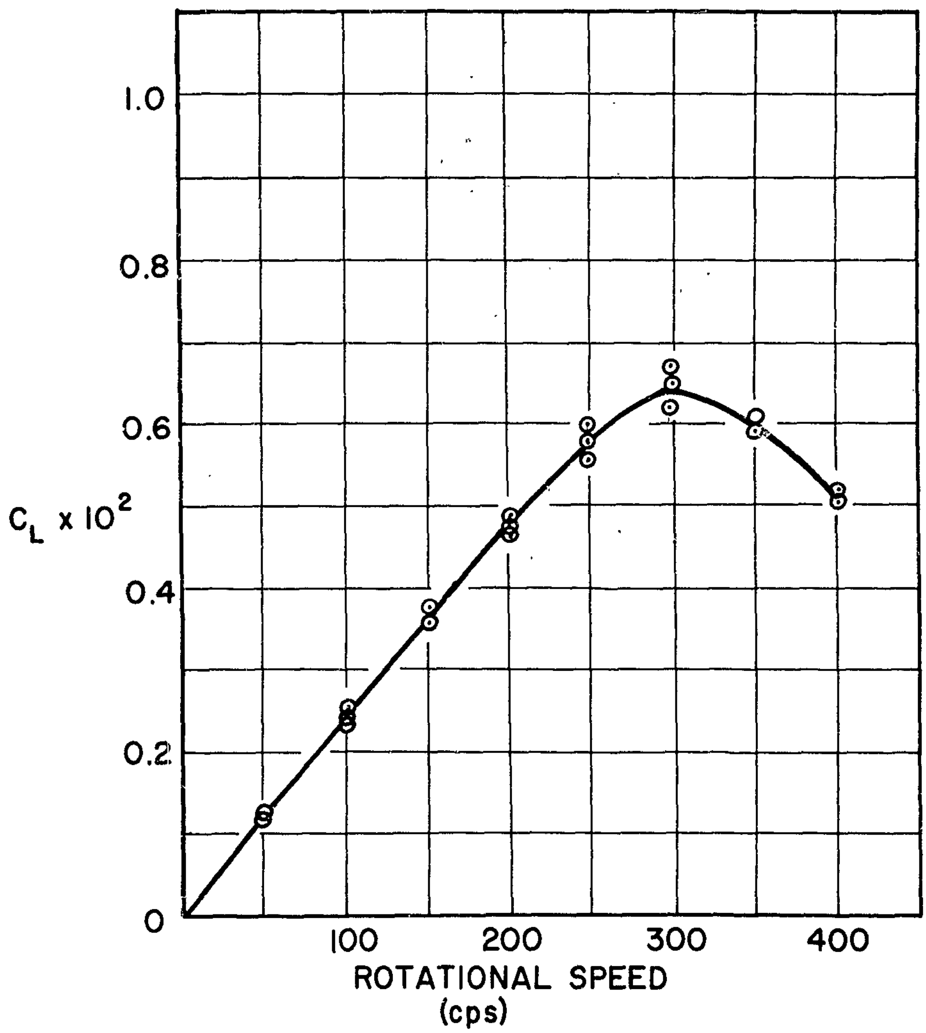

FIG. 5

LIFT COEFFICIENT versus ROTATIONAL SPEED

Re = 0.91 x 10

M = 2.15

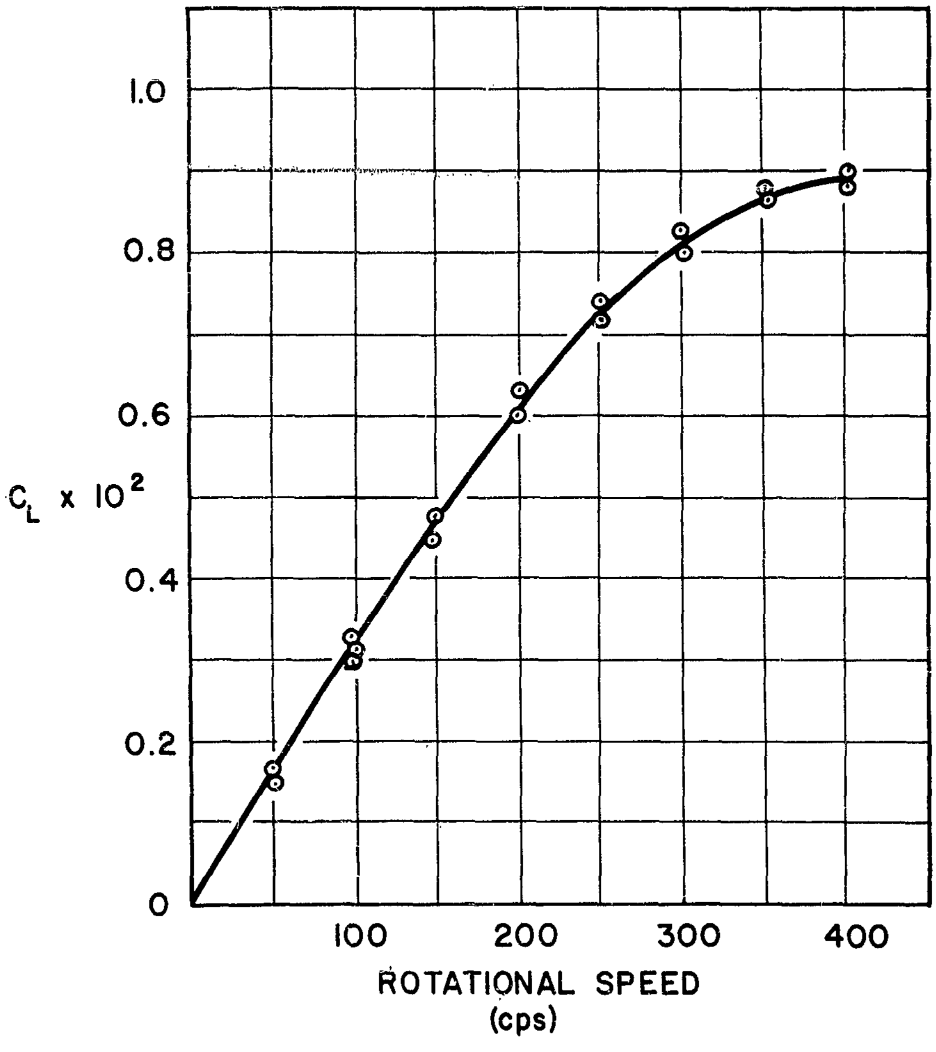

FIG. 6

LIFT COEFFICIENT versus ROTATIONAL SPEED

$Re = 0.78 \times 10^6$

$M = 2.48$

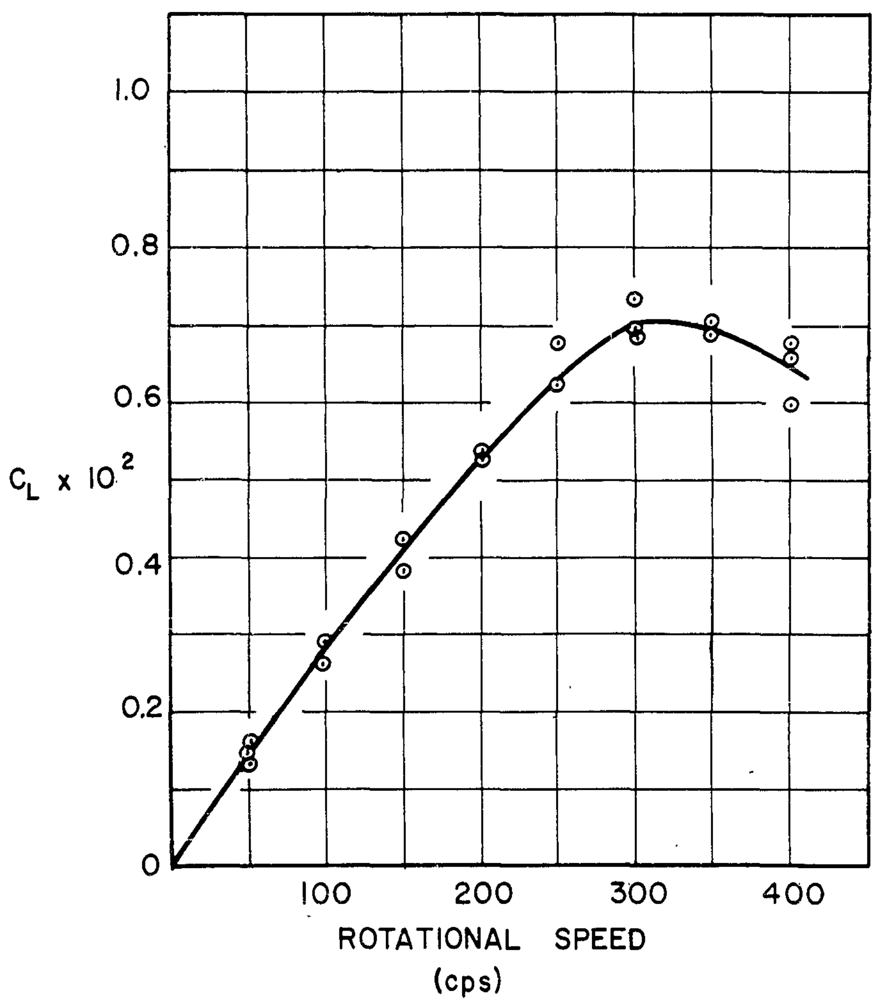

FIG. 7

LIFT COEFFICIENT versus ROTATIONAL SPEED

$Re = 0.55 \times 10^6$

$M = 3.24$

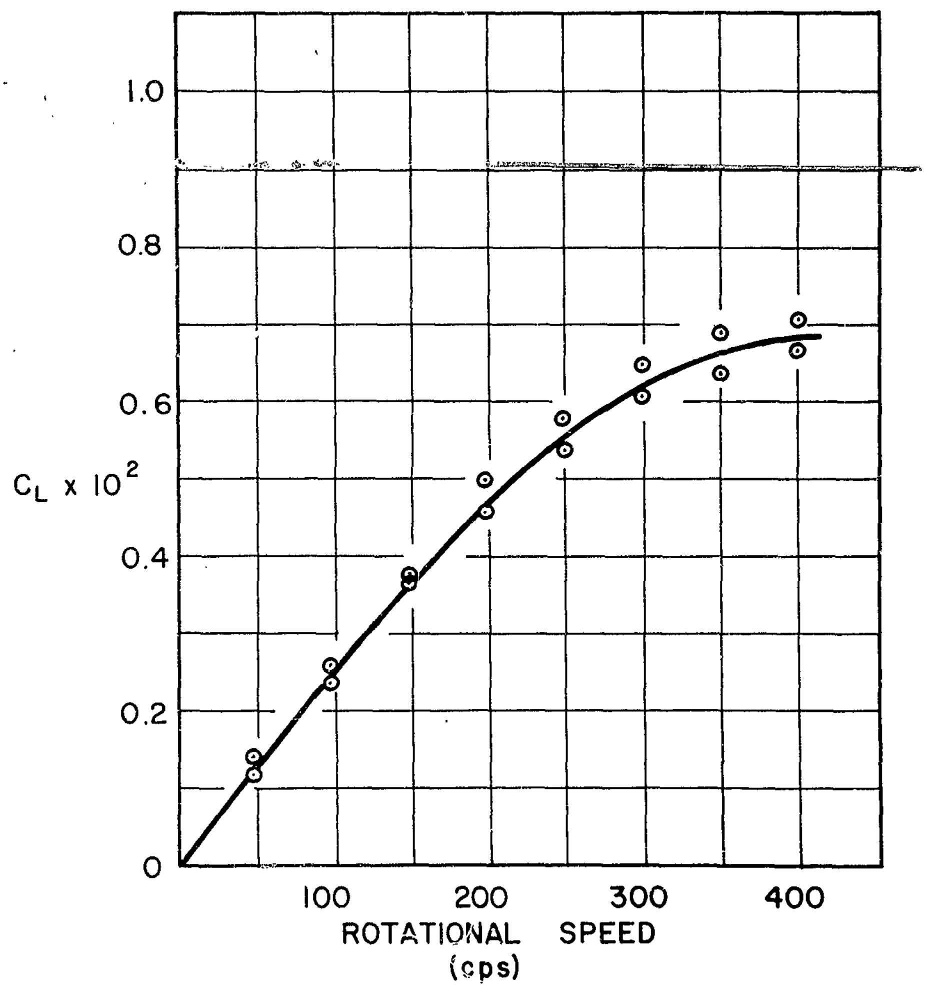

FIG. 8

LIFT COEFFICIENT versus MACH NUMBER

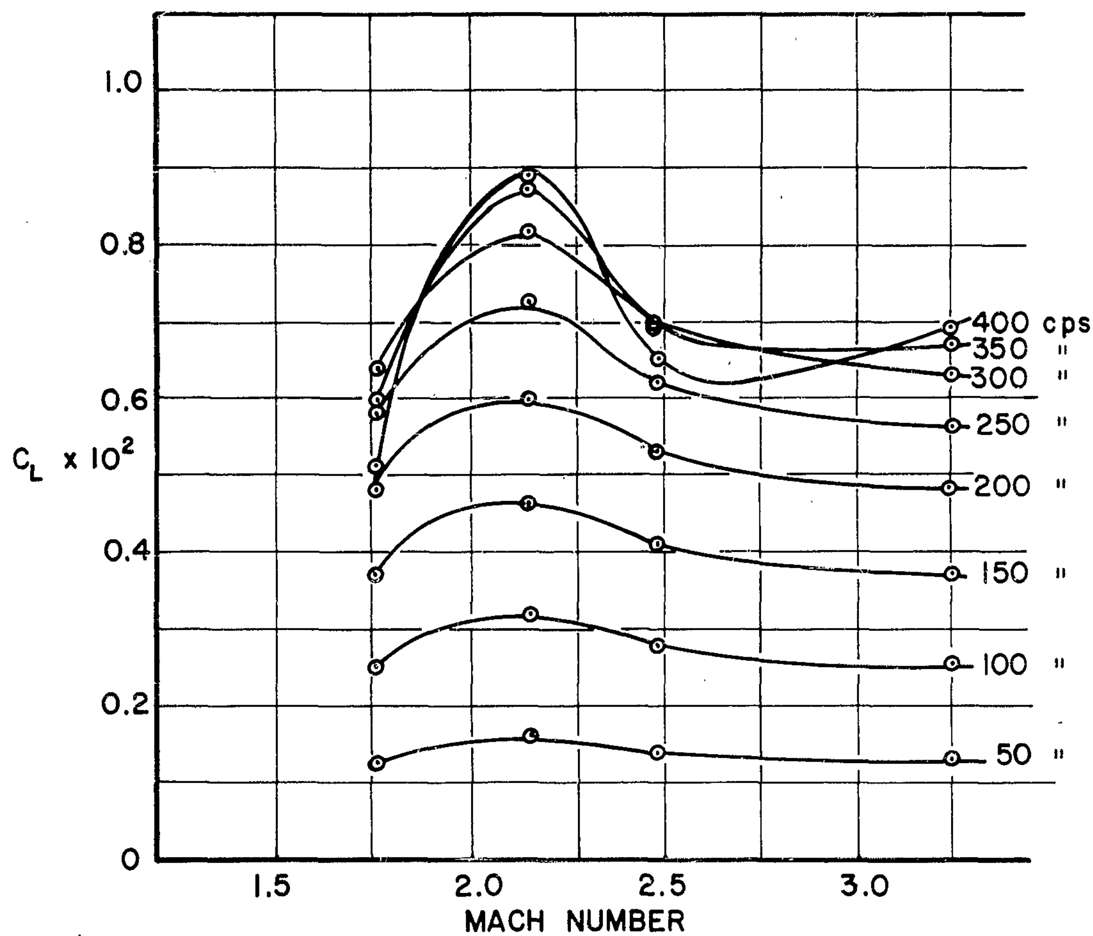

FIG. 9

LIFT COEFFICIENT versus VELOCITY RATIO

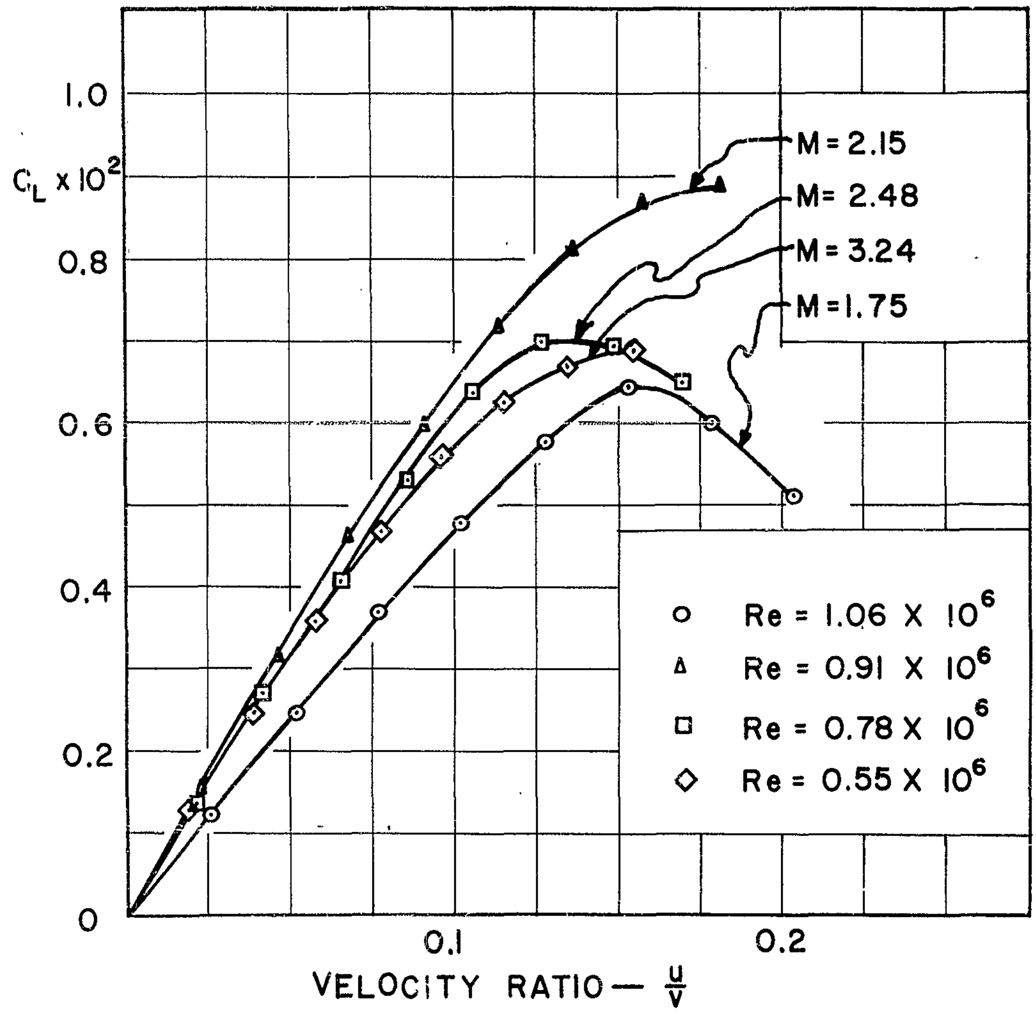

FIG. 10

DRAG COEFFICIENT versus ROTATIONAL SPEED

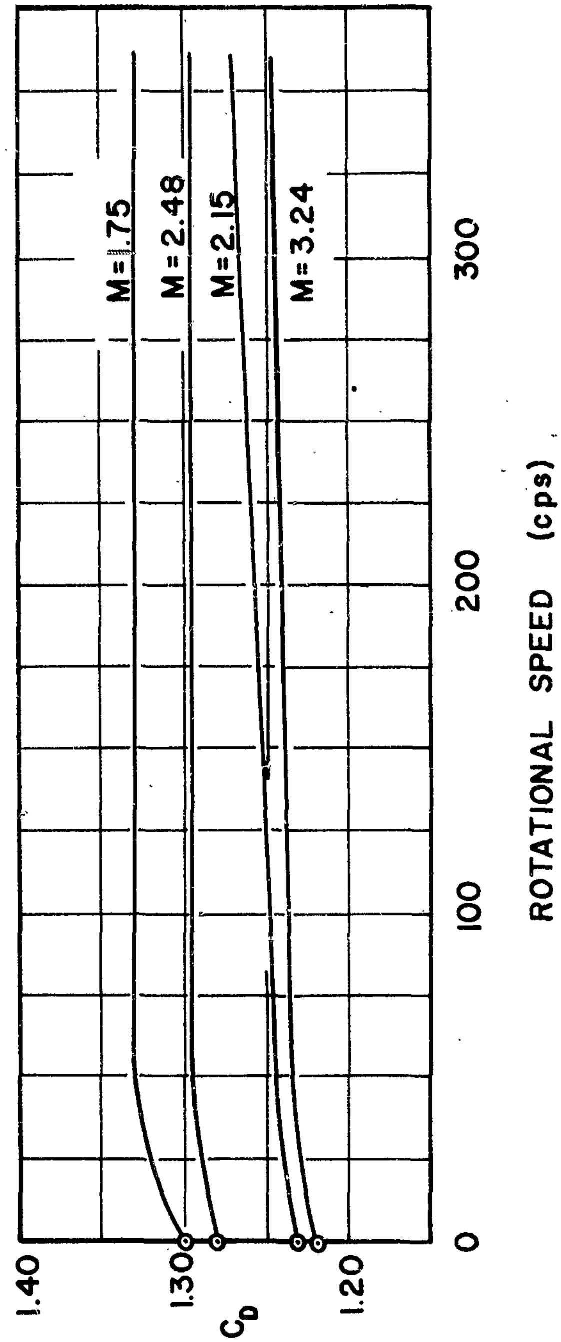

FIG. 11

DRAG COEFFICIENT (NO-SPIN) versus MACH NUMBER

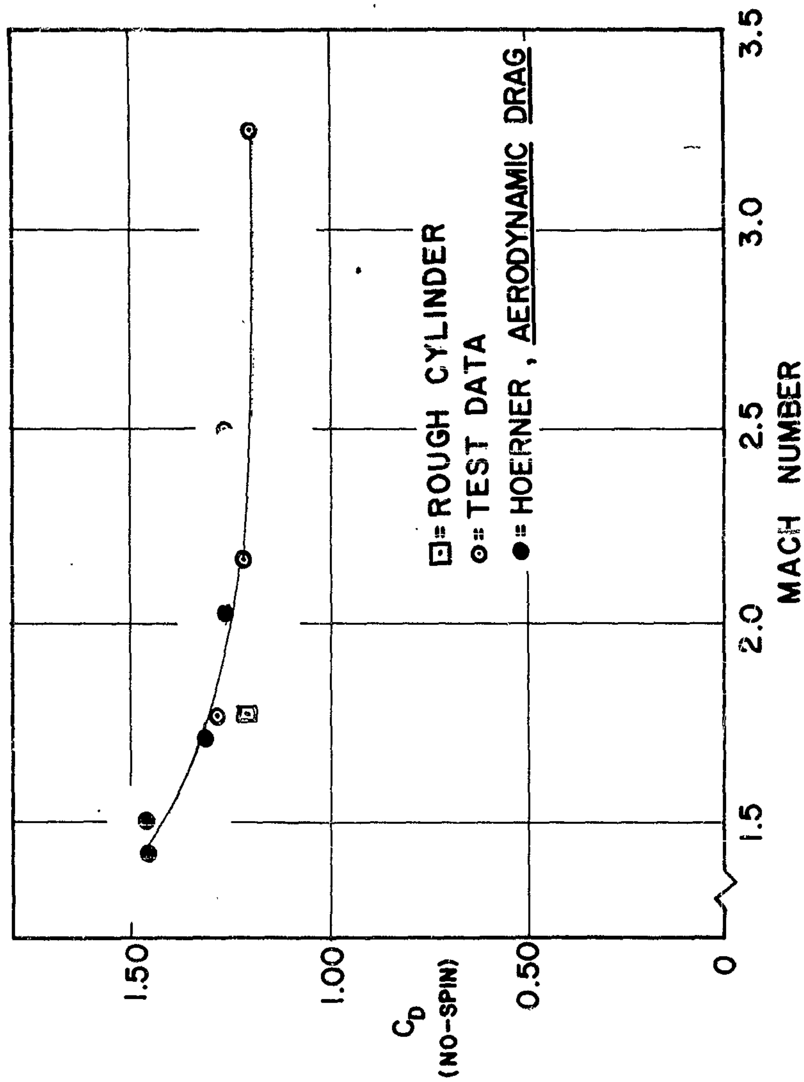

FIG. 12

NAVORD REPORT 6039

LIFT COEFFICIENT versus VELOCITY RATIO

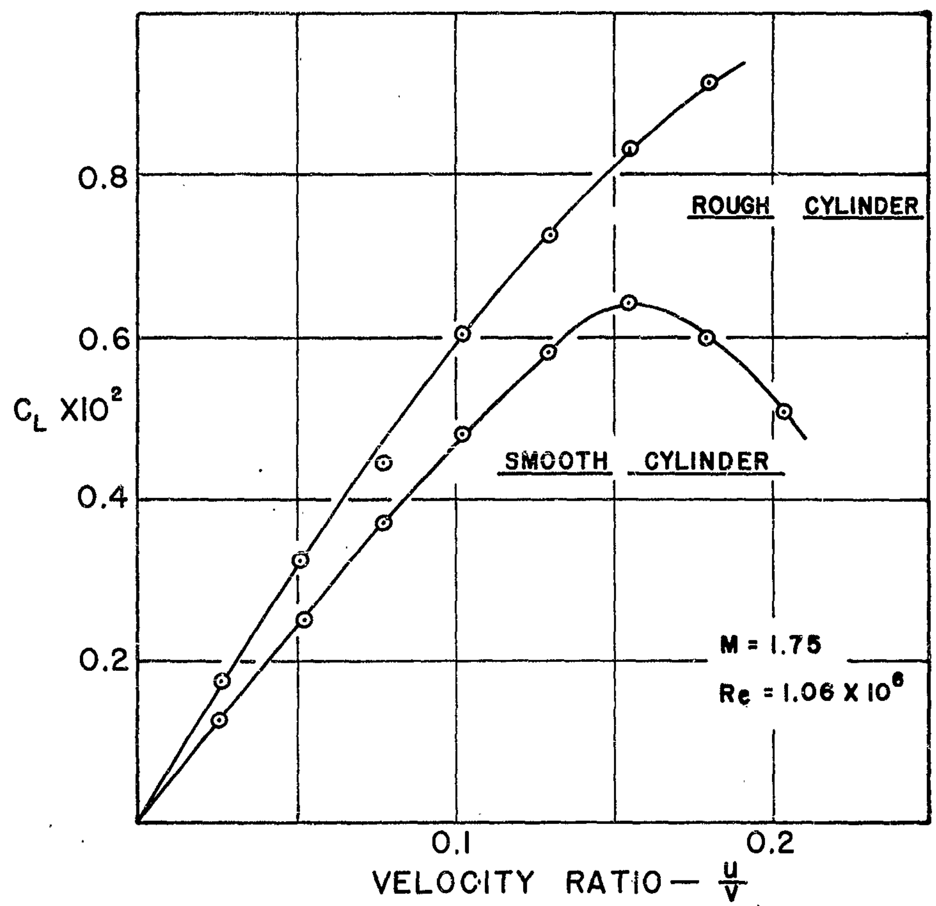

FIG. 13